Journal of NeuroEngineering and Rehabilitation

RESEARCH

Open Access

Insights into the dependence of post-stroke motor recovery on the initial corticospinal tract connectivity from a computational model

Dongwon Kim[1,2,3*], Leah M. O'Shea[1,2,3] and Naveed R. Aghamohammadi[1,2]

Abstract

There is a consensus that motor recovery post-stroke primarily depends on the degree of the initial connectivity of the ipsilesional corticospinal tract (CST). Indeed, if the residual CST connectivity is sufficient to convey motor commands, the neuromotor system continues to use the CST predominantly, and motor function recovers up to 80%. In contrast, if the residual CST connectivity is insufficient, hand/arm dexterity barely recovers, even as the phases of stroke progress. Instead, the functional upregulation of the reticulospinal tract (RST) often occurs. In this study, we construct a computational model that reproduces the dependence of post-stroke motor recovery on the initial CST connectivity. The model emulates biologically plausible evolutions of primary motor descending tracts, based on activity-dependent or use-dependent plasticity and the preferential use of more strongly connected neural circuits. The model replicates several elements of the empirical evidence presented by the Fugl-Meyer Assessment (FMA) subscores, which evaluate the capabilities for out-of-synergy and in-synergy movements. These capabilities presumably change differently depending on the degree of the initial CST connectivity post-stroke, providing insights into the interactive dynamics of the primary descending motor tracts. We discuss findings derived from the proposed model in relation to the well-known proportional recovery rule. This modeling study aims to present a way to differentiate individuals who can achieve 70 to 80% recovery in the chronic phase from those who cannot by examining the interactive evolution of out-of-synergy and in-synergy movement capabilities during the subacute phase, as assessed by the FMA.

Index terms Stroke, Corticospinal tract, Reticulospinal tract, Fugl-Meyer assessment, Synergy

*Correspondence:
Dongwon Kim
dkim04@sralab.org
[1]Shirley Ryan AbilityLab, Chicago, IL, USA
[2]Department of Biomedical Engineering, University of Illinois at Chicago, Chicago, IL, USA
[3]Department of Physical Medicine and Rehabilitation, Northwestern University, Chicago, IL, USA

Introduction

Clinical observations suggest that the extent of potential motor recovery following stroke primarily depends on the residual connectivity of the ipsilesional corticospinal tract (CST) observed within the first few weeks [5, 66, 67]. The ipsilesional CST is the primary motor descending pathway that conveys motor commands to motoneurons [49]. Stroke survivors generally fall into two groups: one group significantly recovers to the level of mild impairment with substantial hand/arm dexterity, and the other group remains at the level of severe-to-moderate impairment, limiting the restoration of hand/arm dexterity [11]. The success or failure to retrieve hand/arm dexterity may depend on whether CST connectivity is resilient during the subacute phase where spontaneous motor recovery occurs [62]. If CST connectivity is not resilient, alternative pathways, including the contralesional reticulospinal tract (RST), may be employed, leading to improvements in gross motor function [10, 15, 62].

The proportional recovery (PR) rule was not originally devised to account for the initial CST connectivity in motor recovery post-stroke [68]. However, this rule is known to broadly differentiate individuals with stroke into two groups: one group with sufficient initial CST connectivity (fitters) and one group with insufficient or no initial CST connectivity (non-fitters) [5]. The PR rule describes that individuals spontaneously recover an average of 70–80% from the first week of stroke to the follow-up (typically 3 or 6 months) in terms of the Fugl-Meyer assessment (FMA) total score, regardless of sex, age and race [46, 72, 74]. Though there are questions about the PR rule due to issues such as mathematical coupling [28], this rule emphasizes the influence of the initial connectivity of the CST, distinguishing 'fitters' from 'non-fitters'. Fitters achieve 70 to 80% recovery, typically surpassing the threshold of the FMA total score of 40 ~ 42 [33, 64], achieving substantial spontaneous recovery of hand/arm dexterity upon entering the chronic phase. The CST is assumed to be the dominant motor descending pathway in fitters. Meanwhile, non-fitters fail to achieve 70 to 80% recovery. The main reason may be that out-of-synergy test items that require the sufficient functional capability of the CST are difficult for non-fitters to score well on (i.e. Score "2" for each test item) [18, 39, 64]. The CST in this group barely achieves a functional capability level that allows for restoring of hand/arm dexterity.

In this study, we construct a computational model to explain the differential motor recovery of non-fitters versus fitters. This model evaluates how the degree of the initial CST connectivity impacts motor recovery after stroke. We reproduce several key features of subscore distributions of the FMA for the upper extremity in fitters and non-fitters. This allows us to gain insight into the interactive evolutions of motor tract (i.e. CST and RST) dynamics depending on the degree of the initial CST connectivity post-stroke. The subscores of the FMA, derived from 27 subtests for in-synergy and out-of-synergy movements, reveal clues about the functioning neural substrates, potentially distinguishing uses of the CST and RST. We apply a strict assumption that while the type of in-synergy movements (tested using the flexion synergy and extension synergy test items) is mediated primarily by either the CST or RST, the type of out-of-synergy movements (tested using the synergy-mixing and out-of-synergy test items) is mediated predominantly by the CST. Individuals with no neurological deficit can conduct elbow flexion while performing shoulder abduction (which is considered as an abnormal synergistic movement following a stroke) by exciting the biceps and abductors individually (via the CST); they do not use involuntary coactivation to perform the movement. We incorporate a stochastic gradient descent algorithm into the Hebbian theory to reflect activity- or use-dependent plasticity [19]. This algorithm successfully replicated the evolution of the torque generation of the elbow joint during flexion, indicating upper- extremity functional activity following stroke. It also revealed that more strongly connected motoneurons are optimized with priority (Reinkensmeyer, Guigon, and Maier [56]). We aim to present a way to differentiate individuals who can achieve 70 to 80% recovery in the chronic phase from those who cannot, by examining the interactive evolution of out-of-synergy and in-synergy movement capabilities during the subacute phase, as assessed by the FMA. Our efforts in this study will provide insights into clinically observed motor improvement during the subacute phase and therapy design.

Methods

In this section, we will develop a computational model to simulate how the functional capabilities of the CST and RST interactively change after a stroke using the Hebbian theory, and we will replicate the time evolutions of FMA subscores to verify the model. The difficulty of conducting the instructed movement varies depending on the FMA test items [64]. In particular, performance on out-of-synergy test items largely depends on the functional capability of the CST [64]. We assume that conducting the instructed movement for each test item requires the functional capability of the appropriate motor tract to exceed a certain level (threshold). Also we assume that the neuromotor system predominantly uses a more strongly connected motor tract to achieve a target movement, optimizing this tract further. Conversely, the system cannot achieve the target movement if the capability of the tract does not exceed the threshold.

Tract model development

Throughout this study, tract connectivity describes the degree of tract connection to convey motor commands to innervate the target motoneurons. Tract connectivity, perhaps synonymously used with tract integrity, particularly of the CST, has been well studied with imaging (e.g., diffusion tensor imaging (DTI)) [32, 38] and neurophysiological methods (e.g., transcranial magnetic stimulation (TMS)) [26, 62]. Tract accessibility, on the other hand, reflects that the cortex wires a tract to relay motor commands. Tract functional capability is linked to the capability of performing the target movement using the tract. An improvement in tract functional capability is assumed to be accompanied by improvements in connectivity and accessibility.

Hebb's model [19] is employed to simulate the functional capabilities of tracts. The model encompasses the features of activity- or use-dependent neural plasticity and its accompanying connectivity following a stroke. The following basic equation describes the overall motor capability reflecting the descending pathways' involvements and corresponding neural activities.

$$C_i = \sum_{i=1}^{N} f_w\left(w_i\right) f_x\left(x_i\right)$$

where *C*,*w* and *x* denote the overall motor capability, the weight of a connection and the cell firing rate, respectively. *f* denotes a response function and *N* is the number of cells.

We made several assumptions regarding the equation. Increases in the values of weights are assumed to represent anatomical recovery primarily. The values of firing rates are assumed to primarily represent the effort to achieve an intended motor goal; that is, an appropriate tract is activated by the cortex to relay motor commands (*accessibility*). Those values are thought to also reflect anatomical recovery through cortical reorganization. We assume that weights and firing rates increase as motor execution is repeated based on use-dependent neural plasticity as reported in studies [9, 47]. Employing a stochastic gradient descent method, the weights and firing rates are updated in a manner that adapts according to the overall motor capability, in the following steps [56]:

1. Activate cells with a firing pattern $x_i = x_0 + v_{xi}$ and increase the weight with a pattern $w_i = w_0 + v_{wi}$, where v_{xi}, v_{wi} are random noise, and measure the corresponding C_i.
2. Update the cell activation patterns and weights:

$$x_{i+1} = x_i + g_x\left(C_n - C_i\right) v_{xi},$$
$$w_{i+1} = w_i + g_w\left(C_n - C_i\right) v_{wi},$$

where g_x and g_w denote learning gains (constants) and C_n is the normal overall motor capability before a stroke.

3. Repeat.

In the model, the weights and firing rates are assumed to be updated based primarily on use-dependent plasticity. Those updates reflect the physiological efforts [47, 56] and motor imagery [59, 60], influencing changes in dendrites and activation of neural stem cells [17, 23], leading to recovery post-stroke [11].

Here, we assume that the ipsilesional CST and contralesional RST are the primary descending pathways in individuals with stroke. In our computational model, the overall motor capability is determined by the functional capabilities of the CST and RST, each of which is expressed as follows:

$$C_i = C_{\mathbf{CST}i} + C_{\mathbf{RST}i},$$
$$C_{\mathbf{CST}i} = \sum_{i=1}^{N_{\mathbf{CST}}} f_w\left(w_{\mathbf{CST}i}\right) f_x\left(x_{\mathbf{CST}i}\right),$$

$$C_{\mathbf{RST}i} = \sum_{i=N_{\mathbf{CST}}+1}^{N_{\mathbf{CST}}+N_{\mathbf{RST}}} f_w\left(w_{\mathbf{RST}i}\right) f_x\left(x_{\mathbf{RST}i}\right),$$

where $N_{\mathbf{CST}}$ and $N_{\mathbf{RST}}$ denote the numbers of cells connected to the CST and RST, respectively.

Tract model simulation

Relying on the observation that reticulospinal inputs show an amplitude of 20% as great as the corticospinal inputs [2, 58], we set the ratio of the numbers of cells connected to the CST and RST before stroke as 5:1 for our model, with an assumption that each cell has the same capability. Five-sixth of the total cells, N, are allocated to the cortex area from which the CST originates (i.e. ipsilesional primary motor cortex (M1)). In contrast, we allocate one-sixth to the source areas from which the RST (specifically, cortico-reticulospinal tract) originates. This allocation does not influence the insights we pursue through the model, because our primary focus is on the trends of the time evolutions of those tracts depending on the other tract's status, not on the absolute values that depend on the number of cells. We simulate 120 cells in total (100 CST cells, 20 RST cells). In this simulation, we consider two cases: Minor Damage and Substantial Damage, according to the number of dead cells or dead connections (i.e. zero weight). The Minor CST Damage case is that less than 20% of the cells connected to the CST are dead, which is hypothesized to simulate populations with strong CST connectivity in the acute phase. The Substantial CST Damage case is that 20 ~ 100% of the cells are dead.

The number of the CST cells with zero weights is determined as a random number chosen from a uniform

distribution. The initial values of w and x of the CST for each case are also determined uniformly randomly, within the range of $[\sqrt{\#\ of\ alive\ CST\ cells}/10 - 0.1, \sqrt{\#\ of\ alive\ CST\ cells}/10 + 0.1]$ for both w and x. There is imaging evidence that the contralesional RST is physically damaged in response to stroke [55]. We assume that the initial values of the weights for the RST range between 0.7 and 0.99. The fact that those values are not set as 1 reflects diaschisis, which describes remote effects on structurally-functionally connected brain regions due to stroke [7]. While the impactof diaschisis on the RST is controversial [7, 26], the primary results of our model are not affected. The values of firing rates are set to a low value (0~0.1) for all cases emphasizing weak accessibility to the RST network. We confirm that the values of those parameters do not significantly change the overall features of behaviors of the tract properties. The learning gains for w and x are randomly set between 1.0×10^{-6} and 1.0×10^{-5}. This difference in those values may reflect the differences resulting from the amount of upper-extremity activity according to the degree of impairment [44, 54], as well as, necrotic tissue, edema, and inflammation, which are known to affect recovery [22, 69]. C_n in the stochastic gradient descent law is set as 100, assuming that the neuromotor system aims to return to the original state where the full capability of the CST is used. The response function f is a saturation function that situates values at ± 1.

Empirical evidence

We re-analyzed FMA subscores collected in a longitudinal study [43]. A total of 67 participants with unilateral upper-extremity motor deficits following first-ever stroke were assessed at 2, 4, 6, 8, 12, 16, 20, and 24 weeks after stroke. Motor function undergoes phases of recovery that are not notably affected by types of therapeutic intervention over the first 24 weeks (6 months) after stroke [42]. Those data were collected within ± 3 days for the assessments at weeks 2–8 and ± 1 week for those at weeks 12–24. The percentages of the 67 participants providing data at each time point were as follows: 100% at 2 weeks, 88% at 4 weeks, 82% at 6 weeks, 79% at 8 weeks, 73% at 12 weeks, 67% at 16 weeks, 57% at 20 weeks, and 61% at 24 weeks.

We included participants who completed at least four assessments in our analysis to trace back their motor recovery trends depending on the severity of impairment. We grouped participants into fitters and non-fitters, using our own modified criteria. It is widely accepted that individuals with mild impairment (FMA total score ≥ 43 [73] show substantial arm and hand dexterity, suggesting that the functional capability of the CST is relatively sufficient [33, 34]. We found that individuals who achieve 70% recovery exhibit substantial arm and hand dexterity. Therefore, we regard individuals with FMA total score ≥ 43 in a later phase of stroke (12 ~ 24 weeks) as fitters. In contrast, we regard individuals who fail to achieve 70% recovery and FMA total score beyond 42 in a later phase of stroke (12 ~ 24 weeks). The percentage of recovery is assessed, with some modifications adjusted to our data, based on the PR rule (i.e. change in the FMA total score from the first week of stroke to the follow-up (3 or 6 months)), as (FMA total score in a later phase - FMA total score at 2 weeks)/(66 - FMA total score at 2 weeks), where 66 is the possible maximum total score. The FMA total score in a later phase is calculated as the greatest FMA total score assessed between 12 (3) and 24 weeks (6 months) after stroke.

Reproduction of fugl-meyer subscores

The model assumes that movements of each type (in-synergy or out-of-synergy) for FMA subtests can be achieved if the functional capability of an appropriate tract reaches a certain level. Each test item has a score of 0, 1 or 2. A score of 0, 1 or 2 is awarded as 0: Cannot be performed; 1: Can be performed partially; and 2: Can be performed fully, based on the instruction. Accordingly, a higher score requires a greater functional capability of the corresponding tract.

We assume that while the type of in-synergy movements is mediated by either the CST or RST, the type of out-of-synergy movements is mediated primarily by the CST. The CST enables fine movements by innervating individual muscles separately, while the RST is related to gross movements by innervating muscle groups together. Abnormal co-activation across muscles following stroke may originate from the physical feature of the RST that branches to multiple motoneuron pools across the upper extremity and activates them together when a central command descends [4, 13, 14, 29, 65]. Studies demonstrated that individuals with the functional upregulation of the RST show significantly reduced hand/arm dexterity [10, 33, 34]. In this situation, we assume that in individuals with strong initial CST connectivity, the CST is predominantly used to conduct both types of in-synergy and out-of-synergy movements (fitters). In contrast, in individuals with weak or no CST connectivity right after a stroke, the RST is predominantly used to conduct the type of in-synergy movements, and the CST is predominantly used to conduct the type of out-of-synergy movements (non-fitters). A study showed that elbow flexors (and also finger flexors) are innervated via the CST or RST depending on the initial CST connectivity [62].

100 subjects in each group are simulated to reproduce the time evolutions of the 27 test items of the FMA that evaluate motor function. The 27 test items include in-synergy items (6 flexor synergy, 3 extensor synergy) and out-of-synergy items (3 mixing synergy, 3 little synergy,

5 wrist, 7 hand items) [20]. Subject allocation does not notably affect the results. The initial functional capability of the CST in each subject is determined by the number of dead cells chosen in a uniformly random way, ranging [1 20] for fitters and [21 80] for non-fitters, respectively.

For fitters, the Minor CST Damage case of tract dynamics is used. Based on the empirical data, we found that the difficulty levels of the 9 in-synergy items are not discriminable and set their thresholds for Score "2" as [0.80 0.81 0.82 0.83 0.84 0.85 0.86 0.87 0.88]. The 9 thresholds are randomly re-ordered and applied to each individual. We set the thresholds of the 18 out-of-synergy items for Score "2" as [0.84 0.86 0.88 0.90 0.92 0.94 0.78 0.81 0.84 0.87 0.90 0.93 0.73 0.76 0.79 0.82 0.85 0.88]. The thresholds are randomly re-ordered and applied to each individual. While the thresholds of out-of-synergy items for Score "1" are set by multiplying the threshold of each item for Score "2" with a uniformly random number [0.6 0.9], the thresholds of in-synergy items for Score "1" are set by multiplying each threshold for Score "2" with a uniformly random number [0.6 0.9].

For non-fitters, we take a similar approach, using the Substantial CST Damage case of the tract dynamics. The thresholds of the in-synergy items for Score "2" are set as [0.62 0.77 0.82 0.87 0.90 0.92 0.95 0.97 0.98]. Note that those thresholds are also applied to the RST. The thresholds of in-synergy items for Score "1" are set by multiplying each threshold for Score "2" with a uniformly random number [0.1 0.4]. The thresholds of the out-of-synergy items for Score "2" are the same as those for Score "2" for fitters. The thresholds of out-of-synergy items for Score "1" are set by multiplying the threshold of each item for Score "2" with a uniformly random number [0.6 0.9]. This setting is based on our assumption that in-synergy movements are mediated predominantly by the RST in non-fitters and by the CST in fitters, while out-of-synergy movements are primarily mediated by the CST in both groups.

Results

Tract simulation results --- features of our model

a) Minor CST Damage (less than 20% of the cells connected to the CST are dead): the case corresponds to "fitters" in the PR rule.

The anatomical capabilities of the CST and RST are in a reverse relationship

Studies evidenced that the anatomical capabilities of the CST and RST are in a reverse relationship [25, 36]. Given that the functional capability is nearly proportional to connectivity, Fig. 1 implies that the anatomical capabilities of the CST and RST are in a reverse relationship or "competitive" relationship. We observe time evolutions of the CST and RST of 6 subjects (color relevant), suggesting that a greater CST capability leads to a lower RST capability across trials.

Recovery of a tract follows that of another tract

Figure 1 suggests that the functional capability (and connectivity) of the CST increases along with that of the RST as trials advance. This is in agreement with the findings in [31]. The capabilities of the two tracts improve parallelly, while those at a time point are in a competitive relationship.

The model tends to use a more optimized neural network with priority

The neuromotor system continues to use a more optimized neural network with priority [56]. Figure 2 shows that the neuromotor system in individuals with strong CST connectivity in the acute phase tends to optimize the CST with priority while optimizing the RST to

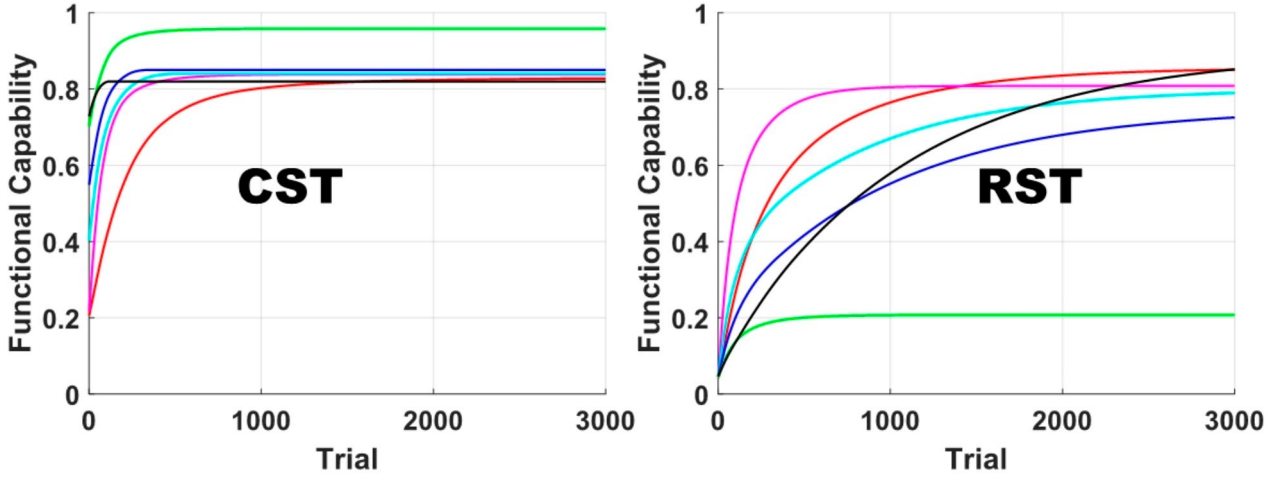

Fig. 1 Functional capabilities of the CST (left) and RST (right) of 6 simulated subjects (color corresponding) across trials (Minor CST Damage case). The learning gains for *w* and *x* vary arbitrarily

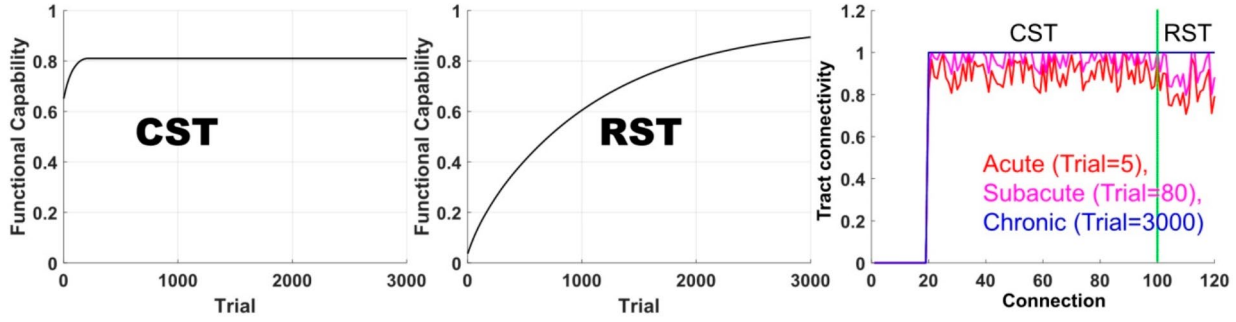

Fig. 2 An example of the functional capabilities and connectivities (values of the weights) of the CST and RST in an individual with strong initial CST connectivity across trials (Minor CST Damage case). We assume that the summation of spinal connection to each cell determines tract connectivity. If a cell is dead, its corresponding connection does not work

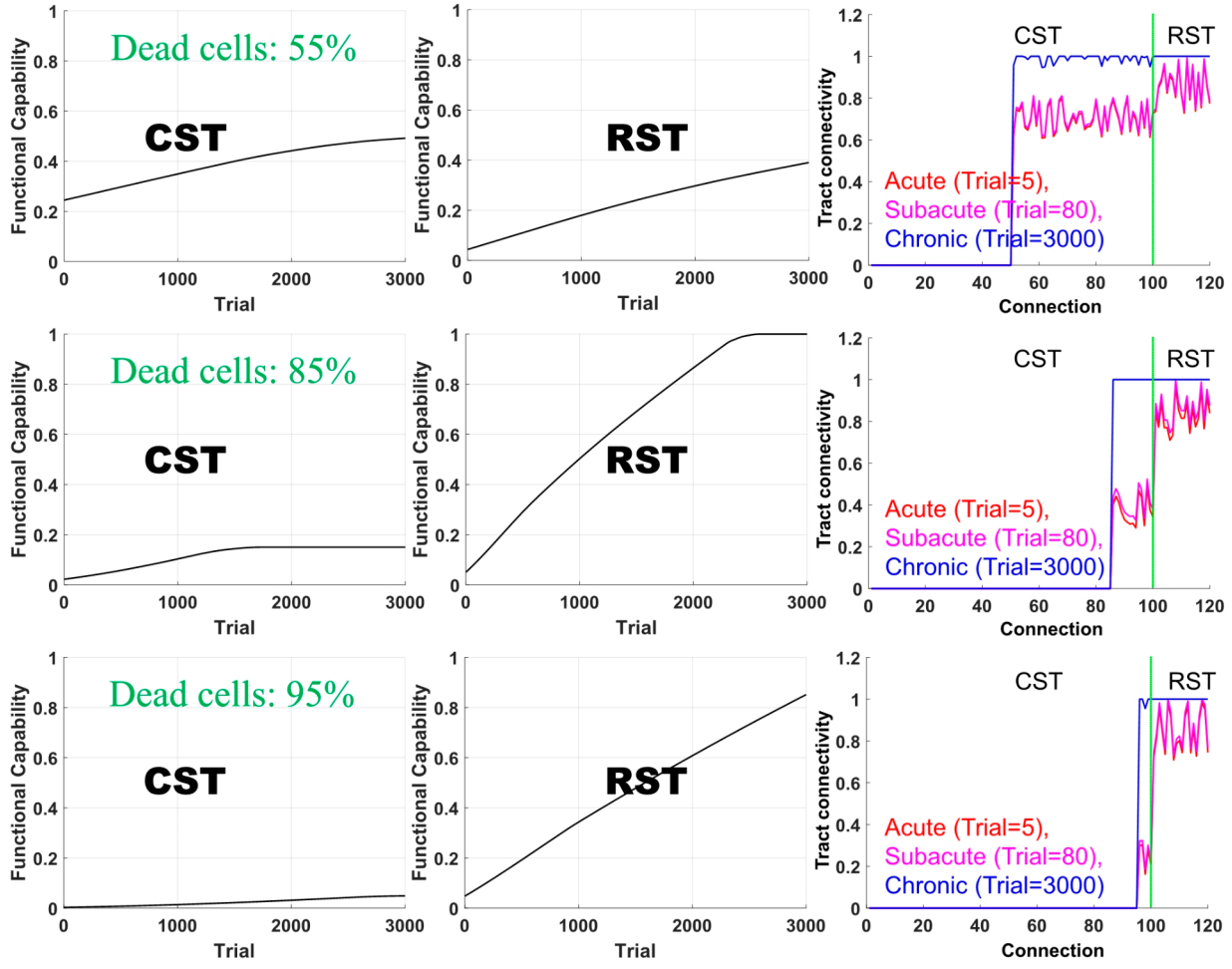

Fig. 3 Examples of the functional capabilities of the CST and RST and connectivities (values of the weights) of the CST and RST in an individual with different numbers of dead CST cells across trials (Substantial CST Damage case). The learning gains for *w* and *x* vary arbitrarily. We assume that the summation of spinal connection to each cell determines tract connectivity. If a cell is dead, its corresponding connection does not work

compensate for the role of the dead CST cells. Meanwhile, Fig. 3 shows that the neuromotor system in individuals in whom RST connectivity is stronger in the acute phase tends to optimize the RST with priority.

CST connectivity in the acute phase is a critical factor for recovery

CST connectivity in the acute phase, measured by TMS, predominantly determines the potential spontaneous recovery [5, 62]. Our results imply that substantial recovery of the CST could be achieved if more than a certain

amount of cells or connections for corticospinal inputs are still alive following a stroke.

b) Substantial CST Damage (20 ~ 100% of the cells): This case decribes phenomena occuring when more than 20% of the CST cells or connections are dead. We assume that the neuromotor system tends to recruit as many as available motoneurons to achieve motor tasks [52]. Since the corticospinal networks become sparse after stroke, the neuromotor system is assumed to optimize the RST network with priority, which is relatively more strongly connected, and then recruit the CST network to achieve the target functional capability to conduct motor tasks. Figure 3 explains this recruitment mechanism. This suggests that the evolution of the functional capacity of the RST varies as a function of the degree of CST lesion and the rate of neural change (i.e. learning gains in the update laws for the cell activation patterns and weights).

Results of FMA subscore analysis

37 fitters (FMA total score ≥ 43 at 12 ~ 24 weeks) were identified, while 20 non-fitters who failed to achieve 70% recovery and FMA total score beyond 42 at 12 ~ 24 weeks were identified. Most of the fitters tend to be near the line of 70% recovery, whereas all non-fitters stay far behind the line, as shown in Fig. 4(a). Figure 4 shows that regardless of the severity of the initial impairment, substantial recovery is achieved in fitters within the first two months. We note that the recovery rates of the types of in-synergy and out-of-synergy movements in fitters are not notably differentiable from each other, suggesting that the CST predominantly mediates both types. Meanwhile, the recovery rates of the types of in-synergy and out-of-synergy movements are relatively slower and notably differentiable from each other, suggesting that different motor tracts mediate both types. These results follow our previous study [33].

Results of FMA subscores reproduction

Figure 5 presents the results reproduced by the proposed model. Successful reproduction suggests that the neuromotor system prioritizes optimizing a more strongly connected motor tract and uses the other tract in a supplementary manner to enhance overall motor capability. In contrast, those two tracts recover in a parallel way. We

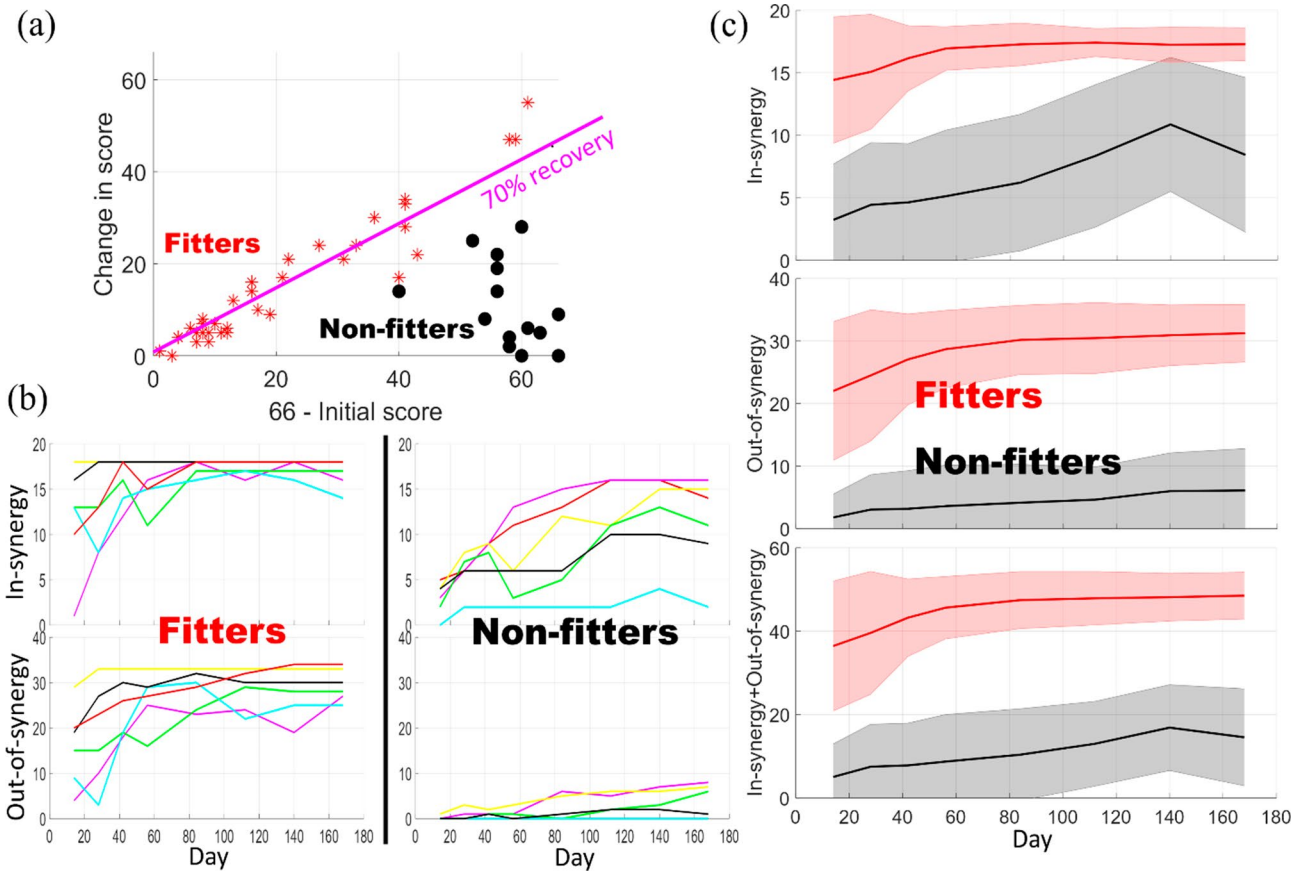

Fig. 4 Empirical results: (**a**) Fitters and non-fitters: fitters (red asterisk) reach 70% recovery or show mild impairment (FMA score ≥ 43) and non-fitters (black dot) do not reach 70% recovery. (**b**) Time evolutions of the total scores of (in-synergy) and (out-of-synergy) test items of 6 representative participants in each group (color corresponding) after stroke. (**c**) Time evolutions of the subtotal scores of (in-synergy), (out-of-synergy), and (in-synergy and out-of-synergy) test items averaged across participants in each group after stroke. Cloud: 1 standard deviation

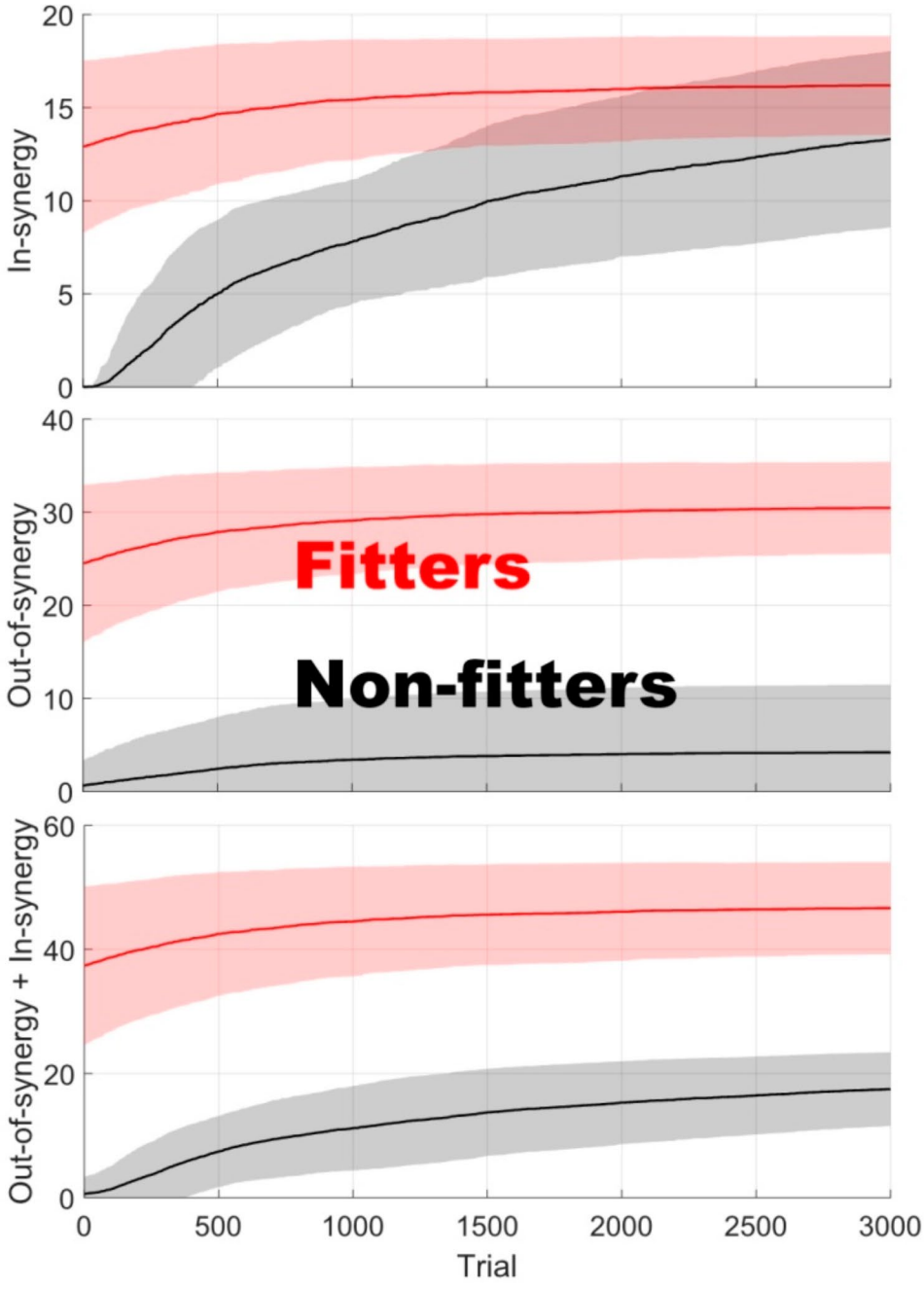

Fig. 5 Simulation results: Time evolutions of the subtotal scores of (in-synergy), (out-of-synergy), and (in-synergy and out-of-synergy) test items averaged across simulated subjects ($n = 100$) in each group (fitters and non-fitters) after stroke. Cloud: 1 standard deviation

found the following observations from model simulation that support empirical phenomena:

1. Fitters reach the plateau of motor recovery within a shorter period than non-fitters [11].
2. The motor function in non-fitters improves at relatively slow and diverse rates [11, 12, 33].

Discussion

Replication of biological mechanisms

This modeling study was initiated based on the primary observations from the PR rule [5]. This was also influenced by the predicting potential for upper limb recovery 1, 2 (PREP 1, 2) algorithms [66, 67], and by a study [62]. Functional recovery post-stroke can be dichotomously differentiated based on the connectivity of the ipsilesional CST assessed within two weeks after a stroke.

Reliance on alternative tracts increases if neural networks along the CST become too sparse or disconnected to convey motor commands to appropriate motoneuron pools. We aimed to describe the selective and competitive relationship between two hypothetically primary descending pathways after stroke, employing Hebb's model, commonly used to model use-dependent neural plasticity [71].

Our model successfully describes a battery of phenomena we commonly observe in individuals affected by stroke. Above all, the model replicates that the degree of the initial anatomical damage to the CST substantially determines the direction of neural recovery (behavioral restitution or compensation). In our model, some cells (i.e. ipsilesional M1 cells) connected to the CST are destroyed and even disabled by stroke (their firing rates are 0) emulating biological systems [16, 63]. Suppose these cells can no longer function and the number of such cells exceeds a certain threshold. In that case, the neuromotor system begins to use relatively more optimized (less damaged) neural pathways to compensate for the role of those cells. The model assumes that corticospinal pathways connected to those cells are accordingly disabled by stroke. This aligns with the PR rule and PREP algorithms, which suggest that the initial anatomical capacity of the CST, measurable with TMS or imaging, determines the degree of potential recovery categorized as "fitters" versus "non-fitters" (PR rule), or "completed, notable" versus "limited, none" (PREP algorithm). If the cells affected by stroke retain some rudimentary function (i.e., their firing rates are not 0), meaning they are not entirely dead, the neuromotor system continues to regrow and strengthen them for motor execution [52], and those cells and their corresponding circuits become re-optimized. This can be described as the Hebbian-type refinement of neural circuits [51]. This cascade is analogous to the typical occurrences post-stroke. Indeed, stroke deprives some neurons of their normal metabolic substrates, causing them to lose function within seconds [53]. Those neurons are unable to maintain their normal transmembrane ionic gradients, eventually leading to apoptotic and necrotic cell deaths [30, 52]. Surviving neurons in the peri-infarct cortical areas with sufficient blood perfusion undergo active structural and functional remodeling [51]. Dendritic growth and axonal sprouting occur to rewire damaged connections or form new connections [52]. Accordingly, motor function recovers and improves; behavioral restitution can be achieved. This suggests that the spontaneous recovery mechanism and use-dependent neural plasticity revive ipsilesional cells or pathways if they survive [52].

Studies reported that individuals with milder impairment show quicker recovery than those with more severe motor impairment [11]. Meanwhile, motor improvement in individuals who are assumed to increase their reliance on alternative tracts continues throughout the first year after stroke. This suggests that it takes longer for individuals with greater impairment to adapt to compensatory mechanisms for the damaged CST and achieve functional fractionation of the alternative neural pathways, in comparison to the use of the recovered CST and ipsilesional hemisphere in individuals with mild impairment. When CST connectivity is deficient, compensatory strategies emerge, including a shift in interhemispheric lateralization towards the contralesional hemisphere and a shift in representational maps around the infarcted zone [52]. Although the neural circuit used as a substitute is relatively intact or less damaged, time is required for adaptation through activity- or use-dependent plasticity. The amount of fractionation correlates with the time since stroke onset [8]. In the model simulation, we described this phenomenon by assuming that the initial RST accessibility is very low (the firing rates of the RST cells were set near $0 \sim 0.1$). The functional capability of the RST begins near 0, regardless of the degree of CST damage caused by stroke (refer to Figs. 1, 2 and 3), so it takes more time for the RST to reach its maximum functional capacity. As a result, motor improvement in individuals for whom the RST acts as the dominant descending pathway tends to be delayed in comparison to those for whom the CST is the dominant descending pathway.

The time evolutions of FMA subscores suggest that the capability of conducting the type of out-of-synergy movements slowly increases in stroke survivors with severe impairment throughout the subacute phase and into the chronic phase (refer to Fig. 4). This implies that the functional capabilities of the CST and RST increase in parallel post-stroke. This observation agrees with imaging studies showing that all tracts tend to recover simultaneously after damage [31]. Branches of the CST to motoneurons controlling the fingers can still function in individuals with severe impairment; those individuals merely show a degraded ability to extend distal joints due to weak CST connectivity or overwhelming abnormal synergies mediated by the RST [1, 35]. However, at the same time, there is the priority in optimization between the tracts. All those results imply that the relatively less damaged RST network is optimized with priority, and the functional capability of the CST may continue to improve in compensation for the residual functional capability, which the RST cannot fulfill solely.

Suggestions for therapy design

Constraint-induced movement therapy (CIMT) is an established rehabilitation approach to promote the recovery of the ipsilesional hemisphere while suppressing contralesional motor drive post-stroke [40]. This therapy effectively reduces maladaptive neural reorganization by

interfering with cortical motor expansion and reducing reliance on the less affected limb [61]. However, some have argued that CIMT can cause maladaptation through functional reinforcement of compensatory motor activity [37]. True behavioral restitution, a return to normal motor patterns with the affected limb [41], requires the recruitment and restoration of the residual ipsilesional hemisphere/CST. In contrast, training of movement within synergy patterns with the affected limb can selectively enhance the structural and functional capabilities of the RST. A study with intact primates showed that strength training with pulling movements enhanced the RST, not the CST [24]. In humans, the RST is predominantly used to excite the biceps on the paretic side post-stroke [62]. Also, strength training with grasping promotes the RST [45].

Our model did not differentiate between the types of movements that cause neural refinement or optimization of a particular tract. We assumed that activity- or use-dependent neural plasticity in our model is achieved with repetitive movements of muscles that can be excited via either the CST or RST. Our primary interest was to examine how the CST and RST interact and evolve, per the hypothesized principle "A tract that is more strongly optimized becomes optimized with priority". Those muscles include shoulder abductors/flexors [21, 27], elbow flexors [62] and finger flexors [2]. Either the corticospinal network or the reticulospinal network is optimized with priority through use-dependent processes by repeating movements with those muscles or imagery movements, depending onthe initial CST connectivity. If the reticulospinal network is optimized with priority, it ultimately facilitates RST upregulation and abnormal synergies.

Abnormal co-activation across muscles may originate from the physical feature of the RST that branches into multiple motoneuron pools across the upper extremity and activates them together when a central command descends [4, 13, 14, 29, 65]. Even in individuals who predominantly use the RST, selective muscle activation may need to require the CST to convey motor commands, instead of the RST. Naturally, its repetition could promote the structural and functional capabilities of the CST and lead to its dominant use. Upper-limb movement away from stereotypical abnormal synergies may be a promising way to achieve behavioral restitution. Training stroke survivors to simultaneously coordinate and synchronize multiple fingers, alleviating the flexion synergy, is effective in improving finger individuation and hand dexterity [48]. This leads to a significant improvement in the FMA score, suggesting that the impairment of the upper extremity is alleviated.

In our model, the functional capability of the CST is limited by the number of cells on the ipsilesional hemisphere that survive after stroke. However, we believe that cortical representations can be reconstituted in the peri-infarct tissue through repetitions of out-of-synergy movement, like in CIMT [61]. It would be worth investigating the effect of inducing the corticospinal network to be optimized with priority in individuals with weak or no initial CST connectivity after stroke through conducting out-of-synergy movements and blocking activities that enhance the reticulospinal network.

Remarks/limitations

We summarize the following four assumptions imposed on the model, which might be limitations of this study:

1) The improvement in motor function requires those in the functional capabilities of the CST and RST (the additive nature of the functional capabilities of the hypothetically primary descending motor tracts).

2) Specificity of the CST to the improvement in scoring in FMA out-of-synergy test items in both fitters and non-fitters.

3) Specificity of the CST to the improvement in scoring in FMA in-synergy test items in fitters.

4) Specificity of the RST to the improvement in scoring in FMA in-synergy test items in non-fitters.

The proposed model is based on Hebbian learning (behavioral improvement) occurring within these predefined assumptions with differential learning rates across (simulated) subjects. The model primarily relies on the thresholds on the CST beyond which the muscles can be innervated. Although we artificially divided the Minor and the Substantial CST Damage cases with a boundary of 20% CST dead cells, it does not influence our results and conclusion. If the functional capability of the CST does not increase beyond the thresholds, the neuromotor system improves the RST to innervate the muscles. For non-fitters, the functional capability of the CST does not reach the thresholds needed to execute a planned movement by innervating the corresponding muscles. Instead, the RST, which is less damaged than the CST, is enhanced to compensate for the role of the CST. They fail to achieve 80% motor recovery. Of course, we assume that all cells and connections have identical capabilities, which may be unrealistic. It is difficult to interpret that the damage size of the corticospinal network can always differentiate non-fitters versus fitters in practice.

This modeling study relies solely on pieces of empirical evidence, not directly measured data. By reproducing the time evolutions of FMA subscores, we tried to infer the motor tract in dominant use and interactive dynamics between the hypothetically primary motor tracts. We assumed that the out-of-synergy movements instructed in the FMA are mediated predominantly via the CST. The type of out-of-synergy movement may be mediated even via the RST, though its execution is weak. We cannot rule out the possibility of functional fragmentation

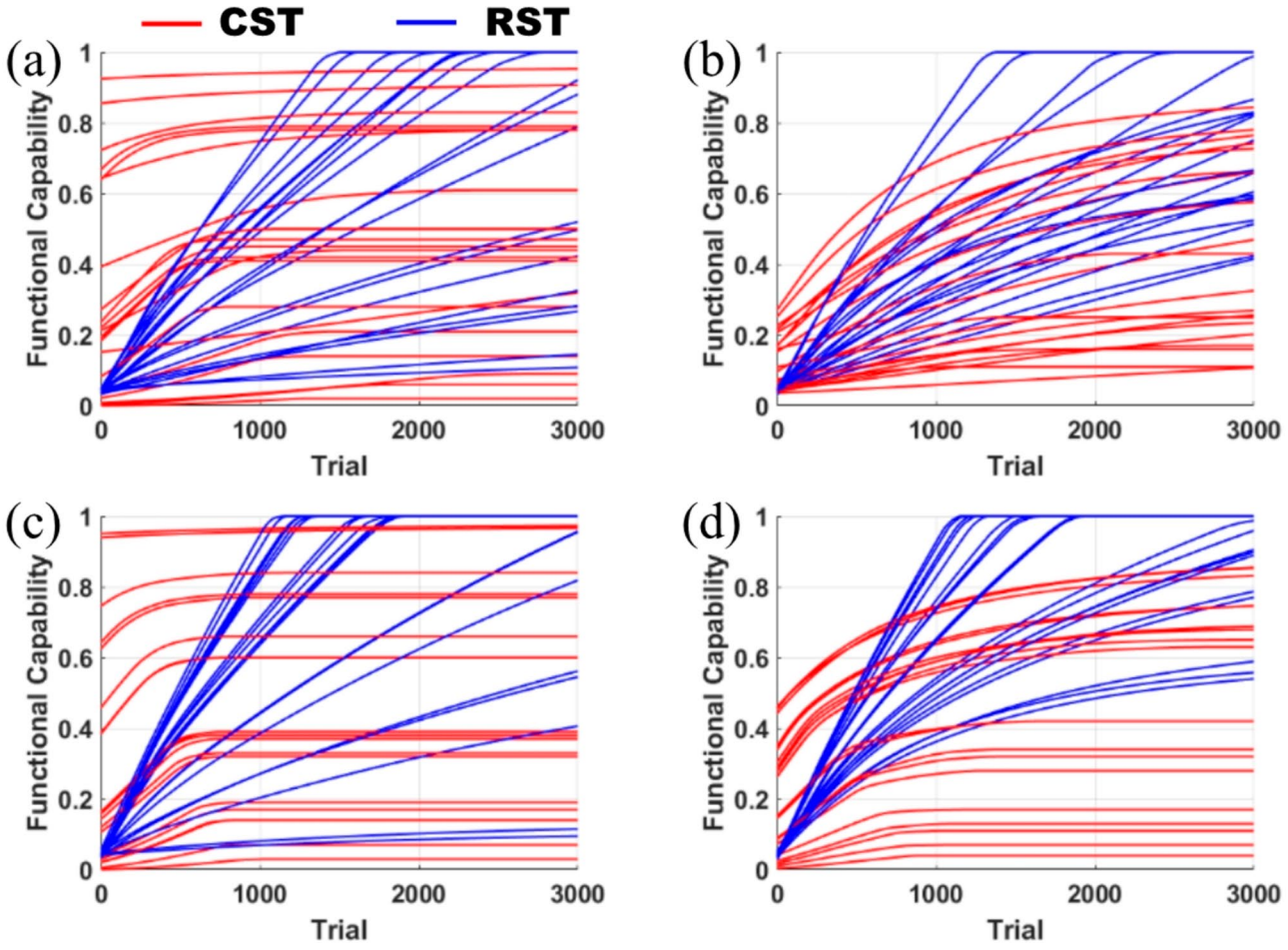

Fig. 6 Time evolutions of the simulated functional capabilities of the CST and RST, with (**a**) the initial values of the firing rate and weight dependent on the number of alive CST cells and the learning gains varying across subjects, (**b**) the initial values independent (randomly chosen between 0.1 and 0.9) and the learning gains varying, (**c**) the initial values dependent and the learning gains fixed, and (**d**) the initial values independent and the learning gains fixed

(remodeling) of the alternative neural substrates (contralesional cortices and RST). Several studies demonstrated that structural reorganization of the contralesional cortices occurs following stroke and contributes to motor improvement, possibly promoting joint individuation [3, 6, 57]. However, studies evidenced that the functional upregulation of the RST leads to substantially reduced hand/arm dexterity (i.e. the capability of performing out-of-synergy movements) [10, 50]. Thus, our assumption is considered reasonable. Also, we assumed that different motor tracts are involved in performing in-synergy and out-of-synergy movements in non-fitters. Our previous study with large databases of FMA subscores revealed that significant asymmetry in scoring between in-synergy and out-of-synergy FMA test items was observed in individuals with severe-to-moderate impairment, whereas symmetry was observed in individuals with mild impairment [33, 34]. This study showed similar results (Fig. 4). Such a reverse relationship in capability between in-synergy and out-of-synergy movements, evidenced in FMA subscore distributions and imaging studies [10, 32], could justify our assumption of the involvements of different motor tracts in performing in-synergy and out-of-synergy movements in non-fitters.

Our computational model of tract dynamics involves several parameters: firing rate, weight and learning gain. We set the initial values of the firing rate and weight to identical random values within a specific range. The range was set as a function of the number of the alive CST cells (i.e. $[\sqrt{\#\ of\ alive\ CST\ cells}/10 - 0.1$, $\sqrt{\#\ of\ alive\ CST\ cells}/10 + 0.1]$). However, setting a specific range does not influence the competitive and parallel relationship between the two tracts. Figure 6 shows the time evolutions of the simulated functional capabilities of the CST and RST, with the initial values of the firing rate and weight either dependent or independent of the number of alive CST cells.

For simplicity, we set the values of the learning gains of the firing rate and weight for the CST and RST to identical random values within a particular range, respectively.

The same range was applied to fitters and non-fitters. Figure 6 shows the time evolutions of the simulated functional capabilities of the CST and RST with the learning gains varying across subjects, in comparison to those with the learning gains fixed across subjects. Variability in the learning gains does not influence the competitive and parallel relationship between the two tracts. Although we set the same ranges for the learning gains in fitters and non-fitters for simplicity, the learning gains can reflect the difference in individuals' capability for neural recovery and plasticity. The majority of individuals with strong initial CST connectivity (i.e. fitters) generally recover an average of 70–80% within 1 or 2 months after stroke, regardless of sex, age, race, and the amount of behavioral effort [46, 72, 74]. However, individuals with weak or no initial CST connectivity (i.e. non-fitters) show relatively large variability in the recovery rate [41, 70]. This large variability possibly originates from factors influencing the rate of neural plasticity, including sex, age, lesion size, fractional anisotropy asymmetry, necrotic tissue, edema, and inflammation, all of which are known to affect post-stroke recovery [22, 69]. Therefore, it is more reasonable to set wider ranges for the learning gains in non-fitters.

In the reproduction of FMA subscores, we adopted several assumptions: (1) each instructed movement of the FMA can be conducted once the functional capability of the CST or RST reaches its corresponding threshold; (2) conducting a movement fully (Score "2") requires a greater functional capability of the dominant tract than is needed for conducting a movement partially (Score "1"); (3) the same thresholds for out-of-synergy movements are applied to fitters and non-fitters; and (4) different thresholds for in-synergy movements are applied to fitters (on the CST) and non-fitters (on the RST). In the current study, the threshold for each instructed movement of the FMA was not determined based on direct empirical evidence. We tuned the values of those thresholds to closely replicate the empirical results shown in Fig. 4, as long as those assumptions remain valid. While the values of the thresholds can slightly alter the amplitude, standard deviation, and shape of the resulting curves, the observation remains unchanged. We confirmed that no other scenarios with different threshold values are possible. Since our empirical data are from a small sample size, which may not represent the entire population, we did not focus on precisely matching the simulation results to the empirical ones.

Acknowledgements
We express our heart-felt gratitude to Dr. Catherine Lang at Washington University School of Medicine in Saint Louis for generously providing her Fugl-Meyer data.

Author contributions
D.K. analyzed data and wrote the main manuscript text L.O and N.A. edited it. All authors reviewed the manuscript.

Funding
N/A.

Data availability
No datasets were generated or analysed during the current study.

Declarations

Ethics approval and consent to participate
The Human Research Protection Office at Washington University in St. Louis, MO approved this study and all participants provided written informed consent.

Consent for publication
All authors agreed on this publication.

Competing interests
The authors declare no competing interests.

Received: 17 August 2024 / Accepted: 25 November 2024
Published online: 20 January 2025

References

1. Baghi R, Kim D, Koh K, Li QZ. 2023. Characterization of the influence of the Dominant Tract on hand closing Post Stroke based on the Fugl – Meyer score. Sci Rep: 1–7.
2. Baker SN. The Primate Reticulospinal Tract, hand function and functional recovery. J Physiol. 2011;589(23):5603–12.
3. Buetefisch CM. Role of the Contralesional Hemisphere in Post-stroke Recovery of Upper Extremity Motor function. Front Neurol. 2015;6(OCT):1–10.
4. Burge R, et al. Incidence and economic burden of osteoporosis-related fractures in the United States, 2005–2025. J Bone Miner Res. 2007;22(3):465–75.
5. Byblow WD, et al. Proportional recovery after Stroke depends on Corticomotor Integrity. Ann Neurol. 2015;78(6):848–59.
6. Cai J, et al. Contralesional Cortical Structural Reorganization Contributes to Motor Recovery after Sub-cortical Stroke: a longitudinal voxel-based Morphometry Study. Front Hum Neurosci. 2016;10(August):8.
7. Carrera E, and Giulio Tononi. Diaschisis: past, Present, Future. Brain. 2014;137(9):2408–22.
8. Casadio M, Tamagnone I, Summa S, and Vittorio Sanguineti. Neuromotor Recovery from Stroke: computational models at Central, Functional, and muscle synergy level. Front Comput Neurosci. 2013;7(JUN):1–14.
9. Chakrabarty S, Friel KM, Martin JH. Activity-dependent plasticity improves M1 Motor representation and Corticospinal Tract Connectivity. J Neurophysiol. 2009;101(3):1283–93.
10. Choudhury S, et al. The relationship between enhanced Reticulospinal Outflow and Upper Limb function in chronic stroke patients. Neurorehabilit Neural Repair. 2019;33(5):375–83.
11. Cramer SC. Repairing the human brain after stroke: I. mechanisms of spontaneous recovery. Ann Neurol. 2008;63(3):272–87.
12. Cramer SC. Recovery after Stroke. CONTINUUM Lifelong Learn Neurol. 2020;26(2):415–34.
13. Davidson AG, Buford JA. Bilateral actions of the Reticulospinal Tract on Arm and shoulder muscles in the Monkey: stimulus triggered averaging. Exp Brain Res. 2006;173(1):25–39.
14. Davidson AG, Bufore JA. 2004. Davidson_2004. *Motor Outputs From the Primate Reticular Formation to Shoulder Muscles as Revealed by Stimulus-Triggered Averaging Adam* 92(1): 83–95.
15. Dewald, Julius PA, et al. Abnormal muscle coactivation patterns during isometric torque generation at the elbow and shoulder in hemiparetic subjects. Brain. 1995;118(2):495–510.
16. Dobkin BH, Thomas Carmichael S. The specific requirements of neural repair trials for stroke. Neurorehabilit Neural Repair. 2016;30(5):470–78.
17. Eyre JA. Development and plasticity of the Corticospinal System in Man. Neural Plast. 2003;10(1–2):93–106.
18. Feng W, et al. Corticospinal Tract Lesion load: an imaging biomarker for Stroke Motor outcomes. Ann Neurol. 2015;78(6):860–70.
19. Friel KM, Chakrabarty S, and John H. Martin. Pathophysiological mechanisms of impaired limb use and Repair Strategies for Motor Systems

after Unilateral Injury of the developing brain. Dev Med Child Neurol. 2013;55(SUPPL4):27–31.
20. Fugl-Meyer AR, Jääskö L, Leyman I, Olsson S. The Post-stroke Hemiplegic patient. 1. A method for evaluation of physical performance. Scand J Rehabil Med. 1975;7(1):13.
21. Fujiwara T, Sonoda S, Okajima Y, Chino N. The relationships between trunk function and the findings of Transcranial Magnetic Stimulation among patients with stroke. J Rehabil Med. 2001;33(6):249–55.
22. Furlan M, et al. Spontaneous neurological recovery after stroke and the fate of the ischemic Penumbra. Ann Neurol. 1996;40(2):216–26.
23. Ganguly K, and Mu ming Poo. Activity-dependent neural plasticity from Bench to Bedside. Neuron. 2013;80(3):729–41. https://doi.org/10.1016/j.neuron.2013.10.028.
24. Glover IS, Stuart NB. Cortical, Corticospinal, and Reticulospinal contributions to Strength Training. J Neurosci. 2020;40(30):5820–32.
25. Hadjiosif AM, et al. Dissociation between abnormal motor synergies and impaired reaching dexterity after Stroke. J Neurophysiol. 2022;127(4):856–68.
26. Hammerbeck U, et al. The strength of the Corticospinal Tract not the Reticulospinal Tract determines Upper-Limb Impairment Level and Capacity for Skill-Acquisition in the Sub-acute Post-stroke Period. Neurorehabilit Neural Repair. 2021;35(9):812–22.
27. Hammerbeck U, Hoad D, Greenwood R, and John C. Rothwell. The Unsolved Role of Heightened Connectivity from the unaffected hemisphere to paretic arm muscles in chronic stroke. Clin Neurophysiol. 2019;130(5):781–88.
28. Hawe RL, Stephen H, Scott, and Sean P. Dukelow. Taking proportional out of stroke recovery. Stroke. 2019;50(1):204–11.
29. Hirschauer TJ, Buford JA. Bilateral force transients in the Upper limbs evoked by single-pulse Microstimulation in the Pontomedullary reticular formation. J Neurophysiol. 2015;113(7):2592–604.
30. Hossmann KA. Pathophysiology and therapy of experimental stroke. Cell Mol Neurobiol. 2006;26(7–8):1057–83.
31. Jang S, Ho, and Sung Jun Lee. Corticoreticular tract in the human brain: a Mini Review. Front Neurol. 2019;10(November):1–9.
32. Karbasforoushan H, Cohen-Adad J, Julius PA, Dewald. Brainstem and spinal cord MRI identifies altered Sensorimotor pathways Post-stroke. Nat Commun. 2019;10(1):1–7.
33. Kim D, et al. Correlations in abnormal synergies between the Upper and Lower extremities across various phases of stroke. J Neurophysiol. 2024a;132(1):87–95.
34. Kim D, et al. Evidence of the existence of multiple modules for the stroke-caused flexion synergy from Fugl-Meyer Assessment scores. J Neurophysiol. 2024b;132(1):78–86.
35. Kim D, Baghi R, Koh K, Li QZ. 2023. MCP extensors respond faster than flexors in individuals with severe-to-moderate stroke-caused impairment: evidence of uncoupled neural pathways. Front Neurol 14.
36. Kim H, et al. Changes in Diffusion Metrics of the Red Nucleus in Chronic Stroke patients with severe Corticospinal Tract Injury: a preliminary study. Annals Rehabilitation Med. 2018;42(3):396–405.
37. Kitago T, et al. Improvement after constraint-Induced Movement Therapy: recovery of Normal Motor Control or Task-specific compensation? Neurorehabilit Neural Repair. 2013;27(2):99–109.
38. Ko SH et al. 2021. Corticoreticular Pathway in Post-stroke Spasticity: a diffusion Tensor Imaging Study. J Personalized Med 11(11).
39. Koch P, Schulz R, Hummel FC. Structural Connectivity Analyses in Motor Recovery Research after Stroke. Ann Clin Transl Neurol. 2016;3(3):233–44.
40. Kwakkel G, et al. The Dutch Brain Foundation (Hersenstichting Nederland), the Lancet Neurol. Lancet Neurol. 2015;14(2):224–34.
41. Kwakkel G et al. 2023. Motor Rehabilitation after Stroke: European Stroke Organisation (ESO) Consensus-based definition and guiding Framework. Eur Stroke J.
42. Kwakkel G, Kollen B, and Eline Lindeman. Understanding the pattern of functional recovery after stroke: facts and theories. Restor Neurol Neurosci. 2004;22(3–5):281–99.
43. Lang CE, et al. Upper Limb performance in Daily Life Approaches Plateau around three to six weeks Post-stroke. Neurorehabilit Neural Repair. 2021;35(10):903–14.
44. Lang CE, Joanne M, Wagner, Dorothy F, Edwards, and Alexander W. Dromerick. Upper Extremity Use in people with hemiparesis in the First few weeks after stroke. J Neurol Phys Ther. 2007;31(2):56–63.
45. Maitland S, and Stuart N. Baker. Ipsilateral Motor Evoked potentials as a measure of the Reticulospinal Tract in Age-related strength changes. Front Aging Neurosci. 2021;13(March):1–11.
46. Marshall RS, et al. Early imaging correlates of subsequent motor recovery after stroke. Ann Neurol. 2009;65(5):596–602.
47. Martin JH, Kathleen M, Friel I, Salimi, and Samit Chakrabarty. Activity- and use-Dependent plasticity of the developing Corticospinal System. Neurosci Biobehav Rev. 2007;31(8):1125–35.
48. Mawase F, et al. Pushing the Rehabilitation boundaries: Hand Motor Impairment can be reduced in chronic stroke. Neurorehabilit Neural Repair. 2020;34(8):733–45.
49. McMorland AJC, Keith D, Runnalls, Byblow WD. A neuroanatomical Framework for Upper Limb synergies after Stroke. Front Hum Neurosci. 2015;9(FEB):1–6.
50. McPherson JG, et al. Progressive Recruitment of Contralesional Cortico-Reticulospinal Pathways Drives Motor Impairment Post Stroke. J Physiol. 2018;596(7):1211–25.
51. Miller KD, Abbott LF, Song S. Competitive hebbian learning through spike-timing-dependent synaptic plasticity. Nat Neurosci. 2000;3:919–26.
52. Murphy TH, and Dale Corbett. Plasticity during stroke recovery: from synapse to Behaviour. Nat Rev Neurosci. 2009;10(12):861–72.
53. Murphy TH, Ping Li K, Betts, and Richard Liu. Two-photon imaging of stroke onset in vivo reveals that NMDA-Receptor independent ischemic depolarization is the Major Cause of Rapid Reversible Damage to dendrites and spines. J Neuroscience: Official J Soc Neurosci. 2008;28(7):1756–72.
54. Noorkõiv M, Rodgers H. and Christopher I. Price. 2014. Accelerometer Measurement of Upper Extremity Movement after Stroke: A Systematic Review of Clinical Studies. *Journal of NeuroEngineering and Rehabilitation* 11(1).
55. Owen MA. Determining the Brainstem's role in loss of Independent Joint Control. in Chronic Stroke. Northwestern University; 2017.
56. Reinkensmeyer DJ, Guigon E, Maier MA. A computational model of Use-Dependent Motor Recovery following a stroke: optimizing Corticospinal activations via reinforcement learning can explain residual capacity and other Strength Recovery dynamics. Neural Netw. 2012;29–30:60–9.
57. Reitmeir R, et al. Post-acute Delivery of Erythropoietin induces stroke recovery by promoting Perilesional tissue remodelling and Contralesional pyramidal tract plasticity. Brain. 2011;134(1):84–99.
58. Riddle C, Nicholas SA, Edgley, Baker SN. Direct and indirect connections with Upper Limb motoneurons from the Primate Reticulospinal Tract. J Neurosci. 2009;29(15):4993–99.
59. Ruffino Célia, Gaveau Jérémie, Papaxanthis C, and Florent Lebon. An Acute Session of Motor Imagery Training induces Use-Dependent plasticity. Sci Rep. 2019;9(1):1–9.
60. Ruffino Célia, Papaxanthis C, and Florent Lebon. Neural plasticity during Motor Learning with Motor Imagery Practice: review and perspectives. Neuroscience. 2017;341:61–78. https://doi.org/10.1016/j.neuroscience.2016.11.023.
61. Sawaki L, et al. Constraint-Induced Movement Therapy results in increased motor map area in subjects 3 to 9 months after Stroke. Neurorehabilit Neural Repair. 2008;22(5):505–13.
62. Schambra HM, et al. Differential Poststroke Motor Recovery in an arm Versus Hand muscle in the absence of Motor Evoked potentials. Neurorehabilit Neural Repair. 2019;33(7):568–80.
63. Sekerdag E, Solaroglu I, and Yasemin Gursoy-Ozdemir. Cell death mechanisms in Stroke and Novel Molecular and Cellular Treatment options. Curr Neuropharmacol. 2018;16(9):1396–415.
64. Senesh MR, and David J. Reinkensmeyer. Breaking proportional recovery after stroke. Neurorehabilit Neural Repair. 2019;33(11):888–901.
65. Soteropoulos DS, Elizabeth R, Williams, Stuart N, Baker. Cells in the Monkey Ponto-Medullary reticular formation modulate their activity with slow finger movements. J Physiol. 2012;590(16):4011–27.
66. Stinear CM, et al. The PREP Algorithm predicts potential for Upper Limb Recovery after Stroke. Brain. 2012;135(8):2527–35.
67. Stinear CM, et al. PREP2: a biomarker-based Algorithm for Predicting Upper Limb function after stroke. Ann Clin Transl Neurol. 2017a;4(11):811–20.
68. Stinear CM, et al. Proportional Motor Recovery after Stroke: implications for Trial Design. Stroke. 2017b;48(3):795–98.
69. Stinear CM, and Winston D. Byblow. Predicting and accelerating Motor Recovery after Stroke. Curr Opin Neurol. 2014;27(6):624–30.
70. van der Vliet R, et al. Predicting Upper Limb Motor Impairment Recovery after Stroke: a mixture model. Ann Neurol. 2020;87(3):383–93.
71. Whitlock JR, Arnold J, Heynen MG, Shuler, Bear MF. Learning induces long-term potentiation in the Hippocampus. Science. 2006;313(5790):1093–97.

72. Winters C, Erwin EH, Van Wegen A, Daffertshofer, Kwakkel G. Generalizability of the proportional recovery model for the Upper Extremity after an ischemic stroke. Neurorehabilit Neural Repair. 2015;29(7):614–22.
73. Woytowicz EJ, et al. Determining levels of Upper Extremity Movement Impairment by applying a cluster analysis to the Fugl-Meyer Assessment of the Upper Extremity in Chronic Stroke. Arch Phys Med Rehabil. 2017;98(3):456–62.
74. Zarahn E, et al. Prediction of Motor Recovery using initial impairment and FMRI 48 h Poststroke. Cereb Cortex. 2011;21(12):2712–21.

Publisher's note